# ISFET Fabrication and Characterization for Hydrogen Peroxide sensing

Pedro H. Duarte[1], Ricardo C. Rangel[1,2], Daniel A. Ramos[1], Leonardo S. Yojo[1], Carlos A. B. Mori[1], Katia R. A. Sasaki[1,3], Paula G. D. Agopian[1,3] and Joao A. Martino[1].

[1] LSI/PSI/USP, University of Sao Paulo, Sao Paulo, Brazil
[2] FATEC-SP, Faculdade de Tecnologia de Sao Paulo, Sao Paulo, Brazil
[3] UNESP, Sao Paulo State University, Sao Paulo, Brazil
e-mail: phduarte@usp.br

***Abstract*— This work presents the Ion-Sensitive Field Effect Transistor (ISFET) fabrication and electrical characterization for hydrogen peroxide sensing. Two configurations were set up to evaluate the devices sensitivity to the concentration of the solution. First, measurements with one electrode in the sample solution (contained over the gate area) were performed, but the results may not be directly related to the characteristics of the solution, due to the prevalence of secondary effects. The second method, using two electrodes in the sample solution, shows a higher sensitivity at increasing hydrogen peroxide concentrations, in smallest intervals when compared to measurements with one electrode.**

***Keywords—ISFET, Hydrogen Peroxide sensing, Biosensor***

## I. Introduction

Among the various types of pH meters available, those based on ion-sensitive field effect transistors (ISFET) have several advantages such as: reduced size and reproducibility [1]. Many prototypes have been developed for the acquisition, processing and transmission of data in the areas of environmental monitoring, in order to obtain information, for example, in biomedical monitoring to optimize the chronic disease control, such as diabetes.

To control chronic diseases such as diabetes mellitus, monitoring blood glucose levels is extremely important. About 422 million people suffer from diabetes and 1.5 million deaths per year are directly related to diabetes [2]. Gradually, engineering advances enable a higher integration of electronic devices and sensors to facilitate this monitoring and improve overall quality of life [3].

One of the glucose sensing methods is to use an enzymatic layer over an ion-sensitive device, such as the Ion-Sensitive Field Effect Transistor [4]. One candidate for this sensitive layer is the Glucose Oxidase (GOx) [5], which catalyzes the oxidation of glucose forming gluconic acid and hydrogen peroxide ($H_2O_2$). When a proper voltage difference is applied across a solution containing hydrogen peroxide, it breaks down into dissolved oxygen ($O_2$), two hydrogen ions ($2H^+$) and two electrons ($2e^-$) [6]. These hydrogen ions change some electrical characteristics of the ISFET, such as the threshold voltage ($V_{TH}$). Therefore, in this case, the threshold voltage shift is related to the hydrogen peroxide concentration generated by glucose oxidation, which is proportional to the glucose concentration of the sample solution.

The ISFET has an equation that defines its threshold voltage [7], like the MOSFET, given as (1):

$$V_{TH} = E_{REF} - \psi + \chi^{sol} - \Phi_{Si} - \frac{Q_{SS}}{C_{ox}} - \frac{Q_{Si}}{C_{ox}} + 2\Phi_F \quad (1)$$

where $E_{REF}$ is the reference electrode potential, $\psi$ is a chemical parameter that varies as a function of the ions present in the solution, $\chi^{sol}$ is the surface dipole potential of the solvent used to make the solution, $\Phi_{Si}$ is the silicon work function, $Q_{SS}$ is the oxide charge density, $Q_{Si}$ is the depletion charge in the silicon, $C_{ox}$ is the gate oxide capacitance per unit area and $\Phi_F$ is Fermi potential. From (1), it is possible to notice the similarities between the threshold voltage of the ISFET and the conventional MOSFET. However, the work function of the metal gate is replaced by $E_{REF} - \psi + \chi^{sol}$, since this metal is substituted by a sample solution and an electrode.

In this paper, the sensing of hydrogen peroxide will be studied, assuming that its breakdown can form $H^+$ and $OH^-$ ions in the sample solution, modifying the pH value of the solution and, therefore, changing the threshold voltage of the ISFET. These results will help to structure the next steps for the fabrication of glucose biosensors.

## II. Fabrication Process

The devices were fabricated in a (25x25) mm² p-type silicon wafer of <100> crystalline orientation, with thickness of 500 µm and sheet resistance of 145.6 Ω/square. Before starting the fabricating process, the samples went through a cleaning step to remove possible metallic contaminants and impurities coming from the air. The complete fabrication process is shown below:

1. Wet thermal oxidation: field oxide formation;
2. Lithography: definition of source and drain regions;
3. Etch using BOE (Buffered Oxide Etch): source and drain opening;
4. N+ diffusion by proximity: source and drain doping (using the Spin-on-Dopant, see section *A*);
5. Lithography and etching: remove oxide over the channel;
6. Oxidation: growth of the gate oxide;
7. Lithography and etching: source and drain opening;
8. Aluminum thermal evaporation;
9. Lithography and Aluminum etching: formation of source and drain contact and
10. Aluminum evaporation on the back of the wafer: substrate contact.

Afterwards, a deposition of an epoxy-based photoresist, SU-8 [8], was made to form micro reservoirs and micro

Digital Object Identifier: 10.29292/jics.v18i1.646

channels to contain and guide the solution only to the sensing area. The formation of the SU-8 film follows the steps:

1. SU-8 Photoresist deposition;
2. Pre-cure stage;
3. UV exposure;
4. Post-exposure curing to evaporate solvent and make the film denser;
5. Revelation using the SU-8 developer and
6. Rinse in isopropanol.

In Figure 1 is possible to observe the resulting wafer. The interferometry method (Filmetrics F40 [9]) was used to measure the field and gate oxide, resulting in (627 ± 4) nm and (20 ± 5) nm, respectively.

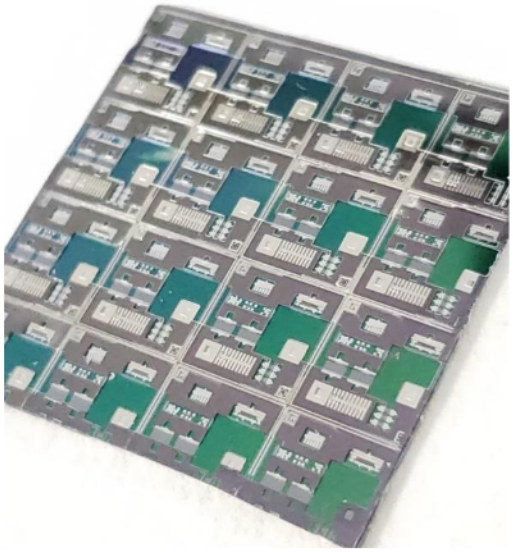

Figure 1. Photo of the fabricated wafer.

The profilometry method was used (Profilometer Dektak 6M [10]) in order to measure the SU-8 thickness, as shown in Figure 2, where it is possible to see that the needle does not touch its own shadow. Although uncommon for this type of measurement, this effect should be expected, given that a relatively thick SU-8 film was formed. Indeed, a value of (145 ± 23) µm for this film was obtained, which is enough to contain the liquids under analysis, as will be shown.

Figure 2. Profilometer measurement of SU-8 thickness.

In Figure 2 is possible to see a cross-bridge structure, which was used to extract the sheet resistance of the $N^+$ diffusion region, resulting in 25.5 Ω/square, and effective $N^+$ diffusion line width ($W_{eff}$) of approximately 40 µm.

Figure 3 shows the ISFETs, with (A) and without (B) the deposition of the sample solution in the gate area. The location of the sample solution only in the gate region means that the SU-8 film was thick enough to prevent overflow, avoiding the contact between the solution and the source and drain pads.

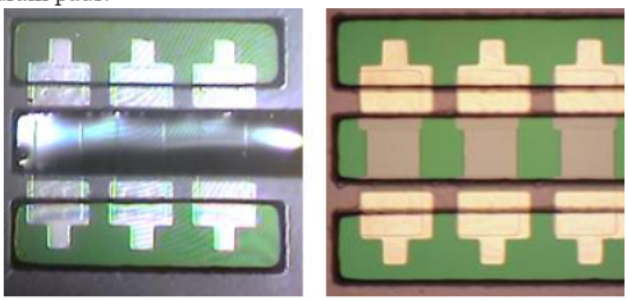

(A) (B)

Figure 3. Fabricated ISFETs with (a) and without (b) the solution in the gate region.

*A. Diffusion by proximity*

There are a few methods of doping silicon wafers to create PN junctions and active regions of transistors. One of the ways to dope wafers is by diffusion, being one of the simplest and cheapest methods to fabricate devices in a university. One way to perform the diffusion process is the spin-on-dopant (SOD) method, which is based on spin-on-glass (SOG). In this method, a liquid containing the dopants is deposited on the sample wafer by a spinner and carry to the oven to be doped. Therefore, the dopant liquid comes into direct contact with the sample wafer. Thus, after the diffusion process, residues of the dopant liquid may remain on the sample, as can see in Figure 4, compromising the functioning of the devices. So, to avoid the problem of the SOD method due to the difficulty of removing liquid source dopant residues when is used, the diffusion by proximity was employed.

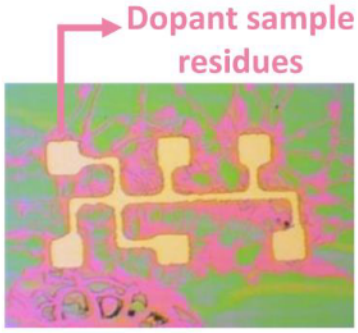


Figure 4. Cross-bridge with dopant sample residues.

To start the process, the liquid source dopant, made at LSI USP [11], is deposited on the surface of a sacrificial wafer, approximately 100 mm of diameter, using the spinner at 2000 rpm for 30 seconds. Next, this wafer is preheated to 200 °C for 15 minutes on a hot plate, in order to evaporate the solvents. Then, it is placed on the carrier approximately 2 mm away from the wafer sample to be doped, as shown in Figure 5. Finally, they are taken to the oven in an environment of $N_2$ at 1150 °C for 30 min. This procedure allows the dopants to diffuse through the environment from the sacrificial wafer to the sample, forming the source and drain regions.

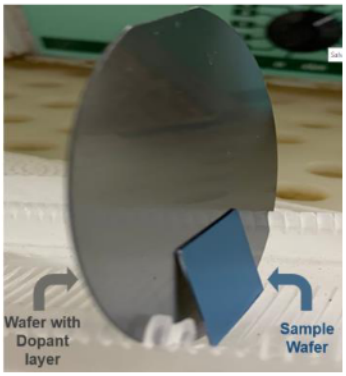


Figure 5. Process of diffusion by proximity.

## III. Electrical Characterization and Results

Two methods were defined to perform the measurement, as the schematic drawn in Figure 6. The method in Figure 6-A uses a single electrode above the ISFET channel to bias the solution, while the method in Figure 6-B employs two electrodes in the solution, with one being on the gate area, effectively acting as the gate, and the second at a distance of approximately 2 mm, connected to the ground.

Figure 7 shows the measurements comparation of (i) a conventional aluminum gate MOSFET, (ii) ISFET with deionized water (DIW) on the gate area using one aluminum electrode, (iii) one platinum electrode, and (iv) using two platinum electrodes.

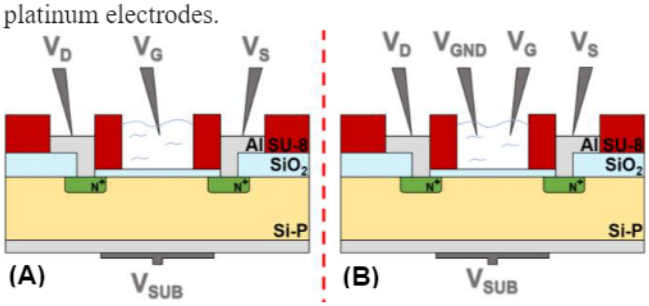


Figure 6. Profile view of the fabricated ISFETs showing two bias methods. The first method (A), only one electrode in the sample solution (gate area) is used. The second method (B), two electrode in the sample solution is used to break $H_2O_2$ molecules.

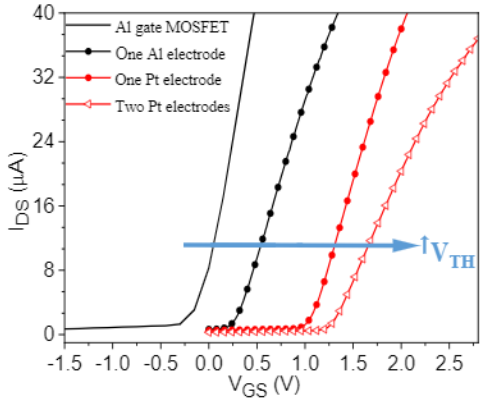


Figure 7. Drain current as a function of gate voltage of conventional transistor, measurement with DIW on the gate of the ISFET using a single electrode of either aluminum or platinum, and a measurement with two platinum electrodes.

Taking the threshold voltage of the MOSFET as the baseline, the threshold voltage shift of the ISFETs under different measurement conditions in Figure 7 may be understood as a direct consequence of equation (1). First, when the aluminum electrode is used, although it is the same material as the metal gate of the reference MOSFET, there is a shift in $V_{TH}$ due to the added effects of $\psi$ and $\chi^{sol}$, as well as a difference between the Al potential operating as an electrode versus its work function. Changing the electrode material to Pt can be understood as a change in EREF, which directly affects the threshold voltage, in this case increasing it, while adding a grounded electrode in the solution may affect the decomposition of the $H_2O_2$ as will be discussed ahead, thus changing possibly both $\psi$ and $\chi^{sol}$, and therefore shifting $V_{TH}$. Since $H_2O_2$ will be present in the solutions to be used from this point on might react with an Al electrode, all further measurements will be performed with the Pt electrodes.

The electrical characterization of ISFETs was performed in the presence of DIW and $H_2O_2$ solutions dissolved in different concentrations in DIW. The voltage applied to the electrode above the gate area ranged from 0 to 2.8 V. The transfer characteristics obtained using one platinum electrode can be seen in Figure 8-A, and the results using two platinum electrodes is presented in Figure 8-B.

Dissimilar behavior of the threshold voltage between the methods is observed. In the first method, the ISFET threshold voltage shifts to more positive values with increasing $H_2O_2$ concentration, while, for the second method, the threshold voltage shifts to more negative values.

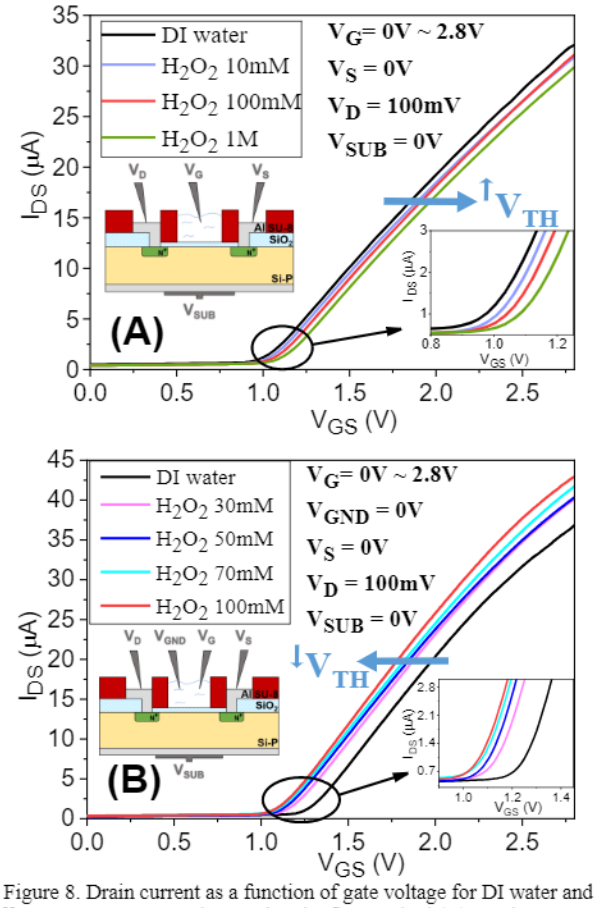


Figure 8. Drain current as a function of gate voltage for DI water and different $H_2O_2$ concentrations, using the first method (A). Drain current as a function of gate voltage for DI water and different $H_2O_2$ concentrations, using the second method (B).

Figure 9 summarizes the threshold voltages extracted with the second-derivative method [12] as a function of the $H_2O_2$ concentration.

Although different concentration intervals were used for each experiment, the total threshold voltage variation for both methods was similar (80 mV over two decades for the first method and 60 mV over approximately half decade for the second method). However, the slope obtained for the first method is greater than that of the second method, indicating that using two electrodes results in a better sensitivity.

Figure 10 shows the sensitivities (S) of the devices, calculated as

$$|S| = \left|\frac{(V_{TH_{SOL}} - V_{TH_{DI}})}{V_{TH_{DI}}}\right| \quad (2)$$

where $V_{TH_{SOL}}$ is the threshold voltage influenced by the $H_2O_2$ solution and $V_{TH_{DI}}$ is the threshold voltage influenced by DIW.

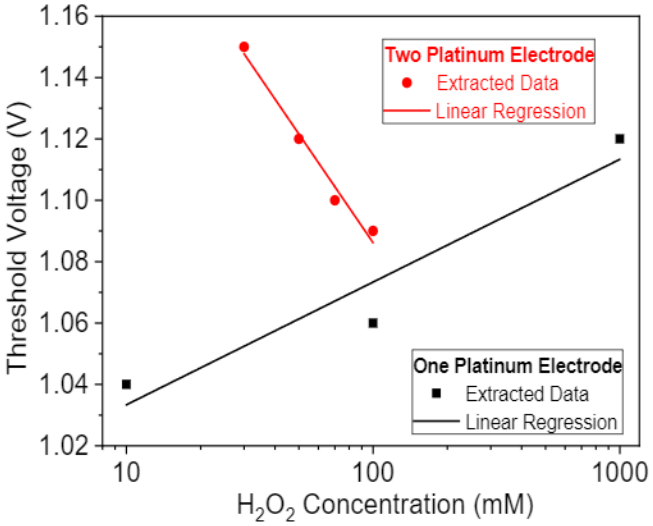


Figure 9. Comparison of the Threshold Voltage ($V_{TH}$) for the two measurement methods.

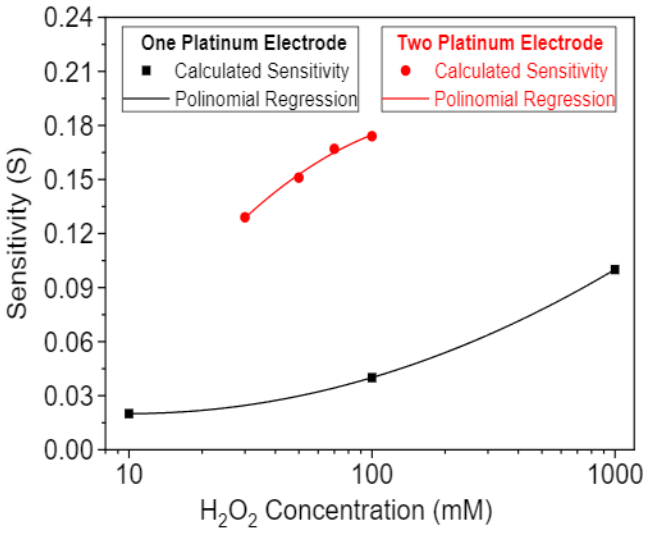


Figure 10. ISFET sensitivity for both methods.

It is possible to observe that the sensitivity for both methods does increase when increasing the concentration of $H_2O_2$, however, using two electrodes provides a higher, and therefore, better sensitivity. This occurs because using one electrode may cause the sensing of other effects that happens in the sample solution. A hypothesis is that the leakage current from the substrate crosses the oxide and reacts with the sample solution over the gate area, modifying the characteristics of the ISFET and making the solution/oxide interface more negative, resulting in a more positive threshold voltage, as shown on the schematic in Figure 11.

For measurements using two electrodes, where a potential difference is applied directly across the $H_2O_2$ solution, the hydrogen peroxide breaks down, forming $H^+$ ions that migrate to the solution/oxide interface. This region becomes more positive, decreasing the threshold voltage, as shown on the schematic in Figure 12.

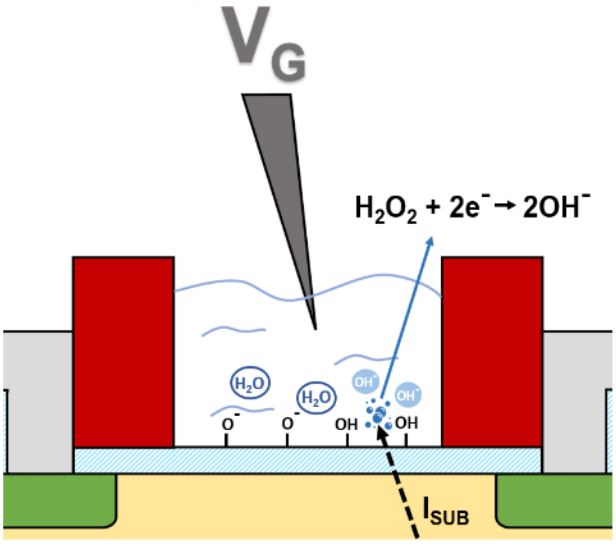


Figure 11. Schematic of threshold voltage change process for the first method.

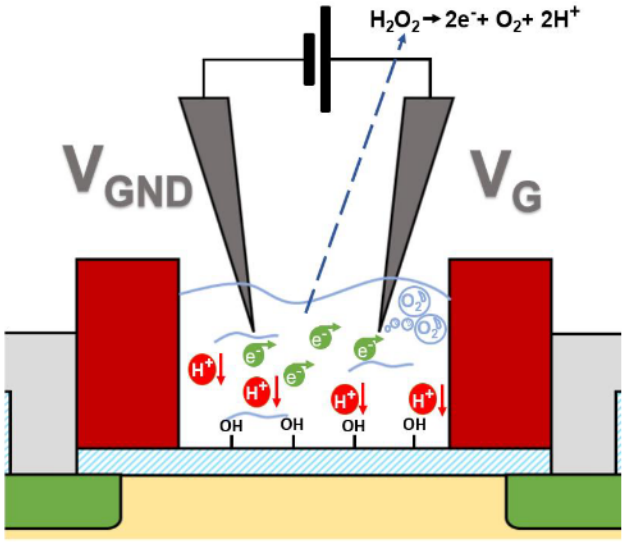


Figure 12. Schematic of threshold voltage change process for the second method.

Furthermore, to corroborate and consolidate the hypothesis that the measurements using two pseudo-electrodes were in fact forming $H^+$ ions, that is, changing the hydrogenic potential (pH) of the solution, experimental measurements were carried out with standard solutions (or buffer solution) of pH.

To make the measurements with the pH solutions, only one electrode was used. The use of two electrodes was only necessary to create a potential difference in the liquid and to

have a current flow between the electrodes to break the $H_2O_2$ molecule and to form ions. However, for pH solutions, there is no need for molecules to break down to form ions, as the solution already contains $H^+$ ions. So, the pH measurement was made with one electrode.

Then, measurements were made with standard pH solutions, from the manufacturers Hanna Instruments® [13] and Dinâmica® [14] with values: 2, 4, 7, 10 and 12. The result obtained can be seen in the graph of Figure 13.

It is feasible that for more basic pH, there is a lower concentration of $H^+$ ions in the solution. That is, the more acidic the pH, the greater concentration of $H^+$ ions can be attracted to the solution/oxide interface. Therefore, it is possible to notice a decrease in the threshold voltage towards a more acidic pH, or even towards higher concentrations of $H^+$ ions in the solution, as seen in the measurements with two electrodes.

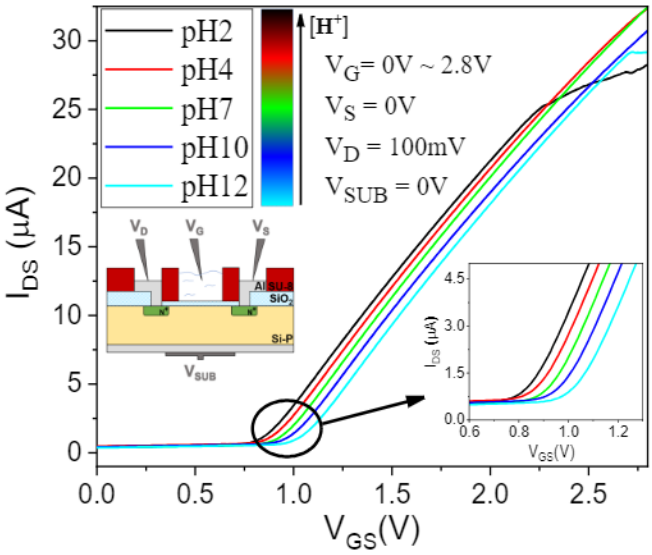


Figure 13. $I_{DS}xV_{GS}$ for measurement of hydrogenic potential (pH) with different concentrations.

## IV. Conclusions

In this work, ISFETs were fabricated and electrically characterized using different solutions in the gate area. For the fabrication of these devices, the proximity diffusion process proved to be simpler and cheaper for the source and drain diffusion step. Furthermore, the deposition of SU-8 to form channels and reservoirs was extremely important to contain the solutions only over the ISFET gate area.

The measurement methods showed different behaviors. If one electrode in the sample solution (gate area) is used, it may present secondary effects that dominate over the $H_2O_2$ influence. On the other hand, measurements with two electrodes in the sample solution promote the breakdown of hydrogen peroxide, resulting in more sensitive and reliable measurements. These results enable the next steps for the fabrication of glucose biosensors to be started.

## Acknowledgements

The authors would like to thank FAPESP, CNPq and CAPES for the financial support.

## References

[1] P. Bergveld. "ISFET, Theory and Practice" IEEE Sensor Conference Toronto, pp. 1-26, October 2003.

[2] World Health Organization, "Diabetes". Available in: <https://www.who.int/health-topics/diabetes>. Access in: April 04, 2022.

[3] J. Kim, A. S. Campbell and J. Wang, "Wearable non-invasive epidermal glucose sensors: A review", Talanta, vol. 177, pp. 163-170, Jan 2018.

[4] V. K. Khanna, A. Kumar, Y. K. Jain and S. Ahmad, "Design and development of a novel high-transconductance pH-ISFET (ion-sensitive field-effect transistor)-based glucose biosensor", International Journal of Electronics, vol. 93, pp. 81-96, 2006.

[5] E.-H. Yoo, and S.-Y. Lee, "Glucose Biosensors: An Overview of Use in Clinical Practice," Sensors, 10(5), pp. 4558-4576, May 2010.

[6] M. Taguchi, A. Ptitsyn, E. S. McLamore and J.C. Claussen, "Nanomaterial-mediated Biosensors for Monitoring Glucose," Journal of Diabetes Science and Technology, 8(2), pp. 403-411, March 2014.

[7] P. Bergveld. "Thirty years of ISFETOLOGY. What happened in the past 30 years and what may happen in the next 30 years?" Sensors and Actuators, vol. 88, pp.1-20, August 2002.

[8] Kayaku. "Technical Data Sheet". Kayaku Advanced Materials, 2020. Available in: <https://kayakuam.com/wp-content/uploads/2020/09/KAM-SU-8-50-100-Datasheet-9.3.20-Final.pdf>. Access in: February 09, 2022.

[9] Filmetrics. "F40 – Thin-Film Analyzer Manual". Filmetrics A KLA Company, 2019.

[10] Veeco. "Dektak 6M Manual" Vecco Instruments, 2006.

[11] A. K. Kawaguti, "Preparação de Fonte Dopante Líquida de Fósforo" Undergraduate thesis. 2015, available in http://biblioteca.fatecsp.br/opac/checkin_form_mono.php?pagina=7, last access in Feb 17, 2022.

[12] A. O. Conde et al, "Revisiting MOSFET threshold voltage extraction methods". Microelectronics Reliability, v. 53, n. 1, pp. 90-104, Jan 2013.

[13] HANNA INSTRUMENTS. pH Solutions. Available in: <https://hannainst.com/ph-solutions>. Access in: May 20, 2022.

[14] DINÂMICA QUÍMICA. Soluções Tampões. Available in: <http://www.dinamicaquimica.com.br/tampoes.php>. Access in: May 20, 2022.